AMERICAN SOCIETY FOR MICROBIOLOGY | Infection and Immunity®

FUNGAL AND PARASITIC INFECTIONS

Role of Calprotectin in Withholding Zinc and Copper from *Candida albicans*

Angelique N. Besold,[a] Benjamin A. Gilston,[b] Jana N. Radin,[c] Christian Ramsoomair,[b] Edward M. Culbertson,[a] Cissy X. Li,[a] Brendan P. Cormack,[d] Walter J. Chazin,[b] Thomas E. Kehl-Fie,[c] Valeria C. Culotta[a]

[a]Department of Biochemistry and Molecular Biology, The Johns Hopkins University Bloomberg School of Public Health, Baltimore, Maryland, USA

[b]Departments of Biochemistry and Chemistry, and Center for Structural Biology, Vanderbilt University, Nashville, Tennessee, USA

[c]Department of Microbiology, University of Illinois Urbana-Champaign, Urbana, Illinois, USA

[d]Department of Molecular Biology and Genetics, The Johns Hopkins University School of Medicine, Baltimore, Maryland, USA

ABSTRACT The opportunistic fungal pathogen *Candida albicans* acquires essential metals from the host, yet the host can sequester these micronutrients through a process known as nutritional immunity. How the host withholds metals from *C. albicans* has been poorly understood; here we examine the role of calprotectin (CP), a transition metal binding protein. When CP depletes bioavailable Zn from the extracellular environment, *C. albicans* strongly upregulates *ZRT1* and *PRA1* for Zn import and maintains constant intracellular Zn through numerous cell divisions. We show for the first time that CP can also sequester Cu by binding Cu(II) with subpicomolar affinity. CP blocks fungal acquisition of Cu from serum and induces a Cu starvation stress response involving *SOD1* and *SOD3* superoxide dismutases. These transcriptional changes are mirrored when *C. albicans* invades kidneys in a mouse model of disseminated candidiasis, although the responses to Cu and Zn limitations are temporally distinct. The Cu response progresses throughout 72 h, while the Zn response is short-lived. Notably, these stress responses were attenuated in CP null mice, but only at initial stages of infection. Thus, Zn and Cu pools are dynamic at the host-pathogen interface and CP acts early in infection to restrict metal nutrients from *C. albicans*.

KEYWORDS calprotectin, *Candida albicans*, copper, nutritional immunity, zinc

Candida albicans is an opportunistic fungal pathogen that normally exists as a commensal organism in the gastrointestinal and genitourinary tracts. Although colonization is normally asymptomatic, *C. albicans* can cause infections in susceptible individuals, including those who are immunocompromised. These infections can range from mild localized candidiasis to severe life-threatening invasive infection in which the fungus enters the bloodstream, ultimately spreading to various organs, including the kidney, liver, and spleen (1).

Like all living organisms, *C. albicans* requires metal micronutrients such as Zn, Cu, Fe, and Mn for vital biochemical processes. *C. albicans* and other pathogenic microbes must acquire these metals from the host, and as part of the innate immune response, the host attempts to limit metal availability through a process known as nutritional immunity (2–5). However, transition metals are also potentially toxic to microbes, and with Zn and Cu there is increasing evidence that the host also exploits toxic levels of these metals in its antimicrobial weaponry (2, 6). In the case of *C. albicans*, host Cu appears dynamic when the fungus invades the kidney in a mouse model of disseminated candidiasis. Kidney Cu is briefly elevated at initial stages of infection, but then,

Received 6 November 2017 **Accepted** 6 November 2017

Accepted manuscript posted online 13 November 2017

Citation Besold AN, Gilston BA, Radin JN, Ramsoomair C, Culbertson EM, Li CX, Cormack BP, Chazin WJ, Kehl-Fie TE, Culotta VC. 2018. Role of calprotectin in withholding zinc and copper from *Candida albicans*. Infect Immun 86:e00779-17. https://doi.org/10.1128/IAI.00779-17.

Editor George S. Deepe, University of Cincinnati

Address correspondence to Valeria C. Culotta, vculott1@jhu.edu.

total kidney Cu falls and the invading fungus reacts by changing expression of Cu-responsive genes, including the *CRP1* and *CTR1* Cu transporters (7, 8). Additionally, *C. albicans* can adapt to low Cu by reallocating intracellular pools of the metal, a process involving repression of the Cu-containing superoxide dismutase *SOD1* and induction of a non-Cu alternative, Mn-containing *SOD3* (7). By repressing *SOD1*, Cu is spared to maintain activity of Cu-dependent cytochrome *c* oxidase, essential for mitochondrial respiration. Sod1 is a major cuproenzyme of the cell, and any loss in Sod1 can be significant in terms of Cu sparing (9). Evidence for such Cu sparing is seen during fungal invasion of the kidney, when *SOD1* expression declines and *SOD3* increases (7, 8). There is also evidence for Zn limitation during fungal invasion of the kidney, whereby *C. albicans* increases expression of genes involved in Zn acquisition, including *ZRT1*, which encodes a Zn transporter, and *PRA1*, which encodes a Zn scavenger, both of which are regulated by the Zn-responsive transcription factor Zap1 (10–12). These indicators of Zn starvation stress suggest that the immune system is withholding this metal from *C. albicans* as it invades the kidney, although the mechanism is not clear.

The immune protein calprotectin (CP) represents one means by which a host can withhold Zn from an invading microbe. CP has been well studied for its Zn-withholding properties from various pathogenic organisms, including Gram-positive and Gram-negative bacteria as well as the fungus *Aspergillus fumigatus*, where a mutant deficient in Zn sensing shows greater susceptibility toward CP *in vivo* (6, 13–18). In addition to Zn, CP can withhold Mn from bacterial pathogens *in vitro* and *in vivo* (13, 14, 16, 19, 20) and can deplete Fe and Ni from specific microbial cultures *in vitro* (21, 22). CP comprises 40 to 60% of the total cytoplasmic protein of neutrophils, accumulates at sites of infection at concentrations of up to 1 mg ml^{-1} (23, 24), and is an important component of neutrophil extracellular traps (NETs) released in the extracellular space during a unique form of neutrophil cell death (25, 26). CP is a heterodimeric protein consisting of S100A8 and S100A9 subunits and acts by binding to extracellular metals using two distinct metal coordinating sites (27). Site 1 (S1) consists of six histidine residues, two from S100A8 and four from S100A9 (28, 29), and has long been known to bind Zn(II) and Mn(II) (28–33) and more recently known to bind Fe(II) and Ni(II) (21, 22). Site 2 (S2) contains a canonical S100 transition metal binding site consisting of two histidines from S100A8 and a histidine and aspartate from S100A9. This site has been termed Zn selective based on its picomolar to nanomolar affinity for this metal, with much weaker affinity for Mn, Fe, and Ni (28, 30, 31, 34, 35). As mentioned above, Cu is another important micronutrient for microbes, particularly eukaryotic microbes (2). To date, CP binding to Cu has not been reported, although fluorescence studies suggest that Cu can induce conformational changes in CP (36), and other S100 proteins, including S100B, S100A12, and S100A13, have been shown to bind this metal ion (37–40), raising the possibility of a role for CP in Cu sequestration.

As with many other pathogens, CP appears to have potent antifungal activity against *C. albicans*. Neutrophil lysates and NETs that are highly enriched in CP are capable of inhibiting *C. albicans* growth *in vitro*, as is purified CP (24, 26, 41–44), and mice lacking CP show a large increase in susceptibility toward *C. albicans* infections in the lung (26). However, the effects of CP on metal starvation stress responses and intracellular metals in *C. albicans* are not known. Moreover, it is currently unknown whether CP is capable of altering metal availability to *C. albicans* inside the animal host.

Here, we investigate the impact of CP on *C. albicans* homeostasis of Zn and Cu *in vitro* and *in vivo*. We observe that when extracellular Zn is depleted by CP, intracellular Zn in *C. albicans* remains remarkably constant and this ability to withstand CP metal withholding is associated with a strong induction of *ZRT1* and *PRA1* Zn uptake systems. We also provide the first direct evidence that CP binds Cu with very high affinity, sufficient to withhold this metal from *C. albicans* and induce the Cu stress response involving *SOD1* and *SOD3*. These transcriptional responses to Zn and Cu limitation *in vitro* were mirrored when *C. albicans* invaded kidneys *in vivo*. The fungal Zn stress response was short-lived and was abrogated in $CP^{-/-}$ null mice. By comparison, the more-protracted Cu stress response was only partly affected by $CP^{-/-}$

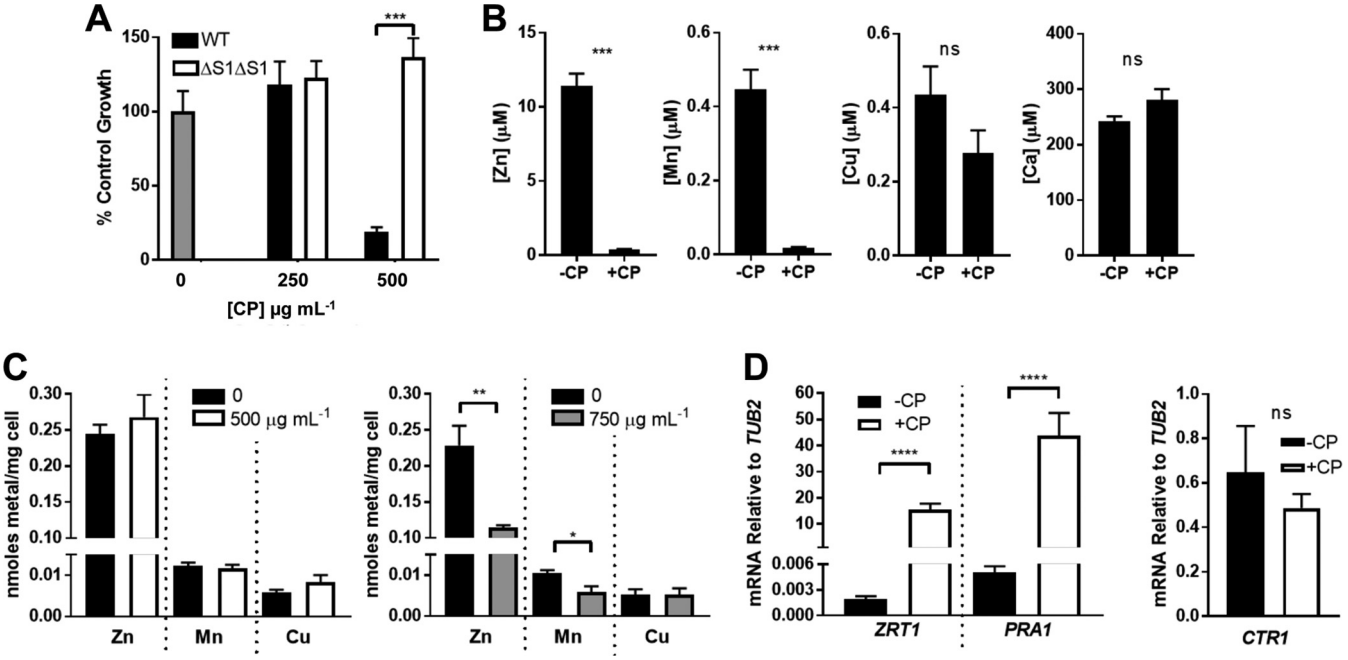

FIG 1 Evidence of CP-induced metal withholding from *C. albicans* in YPD medium. *C. albicans* strain SC5314 was cultured in YPD medium as described in Materials and Methods. (A) Total growth was monitored at OD_{600} for cells grown for 16 h (~12 doubling times) with the indicated concentration of WT or ΔS1ΔS2 CP and is shown as a percentage of untreated control growth (gray bar). Results are averages from four biological replicates over three experimental trials; error bars are standard errors. (B) Metals retained in YPD (no cells) following 7-h treatment with 500 μg ml^{-1} CP were measured as described in Materials and Methods. Error bars represent standard errors from four replicates over two experimental trials. (C) Intracellular levels of the indicated metals were determined as described in Materials and Methods from cells grown for 7 h (~five doublings) with the indicated concentration of WT CP. Error bars are standard errors from 10 (left panel) or four (right panel) biological replicates. There is no significant difference between samples lacking CP (−CP) and those with 500 μg/ml CP for any metal tested or with Cu at 750 μg/ml CP. (D) qRT-PCR analysis of *ZRT1*, *PRA1*, and *CTR1* mRNA levels relative to *TUB2* ($2^{-\Delta CT}$) is shown with cells grown as described for panel C with 500 μg ml^{-1} of WT CP. Error bars are standard errors from 12 (left panel) or 3 (right panel) biological replicates. Significance was determined using a two-tailed *t* test. ****, $P < 0.0001$; ***, $P \leq 0.0002$; **, $P = 0.006$; *, $P = 0.024$; ns, not significant.

mutations and only at early stages of infection. Multiple host factors can contribute to the dynamics of Zn and Cu during infection, and CP specifically functions in early stages to limit metal nutrients from *C. albicans*.

RESULTS

CP withholds Zn from *C. albicans* cultures and induces a Zn starvation stress response in the fungus. Our studies on CP and *C. albicans* were first conducted *in vitro* using laboratory cultures of the fungus and recombinant versions of purified human CP. The experiments whose results are shown in Fig. 1 and 2 used a yeast extract-based medium (YPD) that is standard for laboratory growth of yeast. In this medium, CP exhibited toxicity against *C. albicans* at 500 μg ml^{-1} (Fig. 1A), a concentration within the physiological range of CP (23, 24). To determine the dependence of this growth inhibition on the ability of CP to bind metals, we examined the effects of a CP mutant that cannot bind transition metal ions, termed ΔS1ΔS2. In this mutant, four of the metal binding histidine residues in S1, two from S100A8 and two from S100A9, are mutated to asparagine. In addition, the three metal binding histidine residues and aspartate of S2 are mutated to asparagine and serine, respectively (28). These amino acid substitutions do not perturb the secondary or tertiary structure of CP (30). As seen in Fig. 1A, this ΔS1ΔS2 CP showed no growth-inhibitory effects on *C. albicans*, consistent with the notion that metal binding is linked to the anti-*Candida* activity of CP.

To directly test whether CP is depleting available metals from the growth medium, we adapted the method of Nakashige et al. (21), whereby CP-bound metals are removed by filtration. As seen in Fig. 1B, 500 μg ml^{-1} CP removes over 95% of the soluble Zn and Mn content from YPD medium, while other metal ions such as Cu were not significantly affected. We anticipated that such a dramatic reduction in extracellular Mn and Zn availability would inhibit intracellular accumulation of these metals. Cells

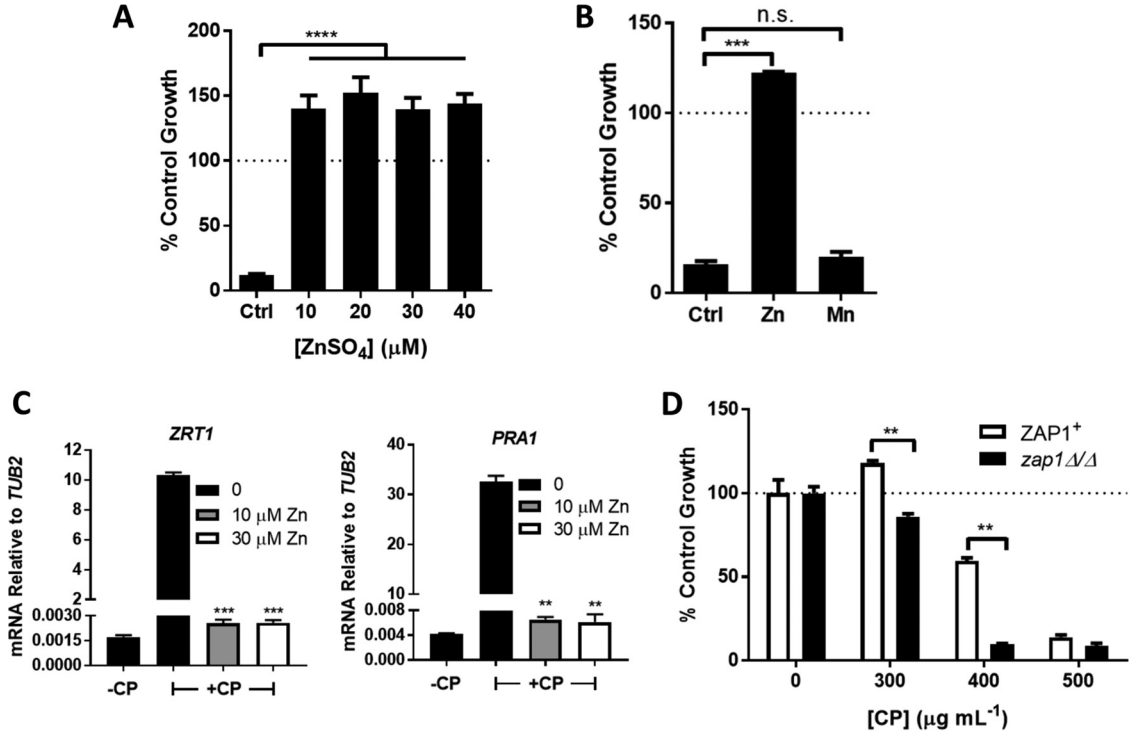

FIG 2 Zn starvation stress and growth inhibition mediated by CP. (A and B) Growth of *C. albicans* SC5314 was carried out and monitored as described for Fig. 1A with 500 μg ml^{-1} CP (20 μM) in YPD medium supplemented with the indicated concentrations of $ZnSO_4$ (A) or 40 μM $ZnSO_4$ or $MnSO_4$ (B). Error bars are standard errors from two to four biological replicates. (C) *ZRT1* and *PRA1* mRNA was analyzed as described for Fig. 1D in *C. albicans* SC5314 grown with 500 μg ml^{-1} CP and the indicated concentration of $ZnSO_4$. Error bars are standard errors for biological duplicates representative of two experimental trials; Zn-treated samples were compared to no-Zn, +CP samples for statistical analysis. (D) *C. albicans strain* SN152 (*ZAP1*$^+$) or the isogenic *zap1*Δ/Δ strain was grown, and data were plotted as described for Fig. 1A. Error bars are standard errors for biological duplicates representative of two experimental trials. Significance was assessed using a two-tailed *t* test. ****, $P < 0.0001$; ***, $P < 0.0003$; **, $P < 0.005$; *, $P < 0.05$.

grown with the toxic dose of 500 μg ml^{-1} CP arrest growth following eight to nine cell doublings (as shown in Fig. 1A), and we sought to examine intracellular metals just prior to this growth arrest, after cells had doubled five times in the presence of CP. As see in Fig. 1C, left, there was no change in intracellular Mn or Zn through numerous cell divisions in spite of the drastic change in extracellular metal availability. Intracellular Mn and Zn were seen to decrease only after treatment with very high levels (750 μg ml^{-1}) of CP (Fig. 1C, right). Thus, *C. albicans* seems quite resilient to the Zn- and Mn-withholding effects of CP through many cell divisions.

Like many microbes, *C. albicans* has evolved sophisticated methods for adapting to changes in extracellular metals by modulating metal transport. Although the systems for responding to Mn limitation are not yet known, the Zn starvation stress response in *C. albicans* has been characterized and involves the induction of *ZRT1*, which encodes a Zn transporter, and *PRA1*, which encodes a Zn scavenger that binds Zn in the extracellular space and delivers it to Zrt1 for import into the cell (12, 45, 46). To test whether this system is activated in *C. albicans* treated with CP, we analyzed the expression of *ZRT1* and *PRA1* by real-time quantitative reverse transcription PCR (qRT-PCR) in cells grown in the presence of 500 μg ml^{-1} CP as shown in Fig. 1C. We observed a very strong induction of both Zn starvation stress genes (Fig. 1D). By comparison, there was no induction of *CTR1*, which encodes the Cu permease (Fig. 1D). The intense induction of Zn acquisition systems with CP may well explain the unchanged intracellular Zn levels over numerous cell doublings despite the dramatic sequestration of extracellular Zn.

What is the cause for growth inhibition following prolonged (more than eight cell doublings) exposure to $\geq$500 μg ml^{-1} CP (as in Fig. 1A)? Previous studies have

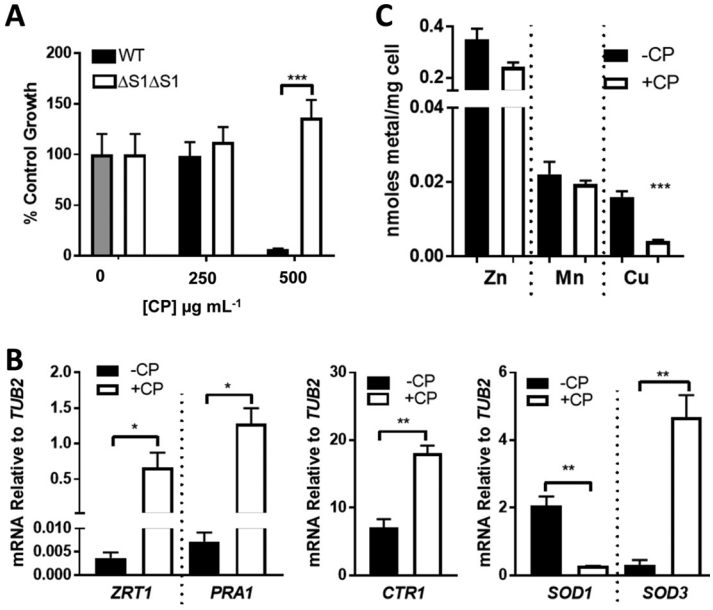

FIG 3 Evidence for CP withholding of Cu from *C. albicans*. *C. albicans* SC5314 was cultured in a medium containing 50% fetal bovine serum based in a low-Cu SC medium (see Materials and Methods). (A) Cell growth in the presence of WT or ΔS1ΔS2 CP was tested as described for Fig. 1A. Error bars are standard errors for four biological replicates. (B and C) Cells cultured where indicated with 500 μg ml^{-1} CP were subjected to mRNA analysis by qRT-PCR (B) or intracellular metals (C) as described for Fig. 1D and C, respectively. Error bars are standard errors from two or three (B) or four (C) biological replicates. Significance was assessed using a two-tailed *t* test. ***, $P = 0.0003$; **, $P < 0.005$; *, $P < 0.05$.

suggested that CP toxicity in *C. albicans* is due to withholding of Zn and/or Mn micronutrients, since supplementation with these metals is able to reverse the anti-*Candida* effects of CP in laboratory cultures (24, 42, 44, 47). Similarly, we observed that supplementation with as little as 10 μM Zn salts completely reversed the growth-inhibitory effects from prolonged incubations with 500 μg ml^{-1} CP (~20 μM) (Fig. 2A). By comparison, four times this level of Mn salts had no effect (Fig. 2B). However, reversal of growth inhibition by Zn supplements is by itself insufficient to demonstrate mechanisms of CP toxicity. The added Zn might also bind to CP and alter its oligomerization state or structure and affect CP activity independent of metal withholding (33, 36, 48, 49). To definitely test whether Zn supplements work by correcting Zn starvation stress in *C. albicans*, we examined biomarkers of Zn deprivation. As seen in Fig. 2C, the induction of *ZRT1* and *PRA1* in the presence of CP was completely reversed by the same Zn supplements that ameliorate CP toxicity.

If intracellular Zn deprivation indeed contributes to the anti-*Candida* activity of CP, the strong induction of Zn transport systems should provide some protection against CP. *ZRT1* and *PRA1* are regulated by the Zap1 transcription factor, and we observed that *zap1*Δ/Δ cells are more sensitive to CP toxicity than the isogenic *ZAP1*$^+$ parental strain (Fig. 2D). All together, the results of *in vitro* culture studies shown in Fig. 1 and 2 indicate that CP has the potential to inhibit *C. albicans* growth through a mechanism involving Zn sequestration; however, the fungus can counteract this effect for a defined period by mounting a Zn starvation stress response involving *ZRT1* and *PRA1*.

CP withholds Cu from *C. albicans* in a serum-based medium. The aforementioned studies were all conducted in a growth medium that is standard for laboratory cultures of *C. albicans* yet is far removed from the physiological habitat of the microbe in the animal host. To better approximate a host environment, we cultured *C. albicans* in animal serum. We observed that the dose response of CP toxicity in cells grown in 50% serum parallels that seen in YPD; moreover, this toxicity is associated with metal binding to CP, as it is reversed by the ΔS1ΔS2 mutant that cannot bind transition metals (Fig. 3A). As expected, 500 μg ml^{-1} CP induced a Zn starvation stress response in

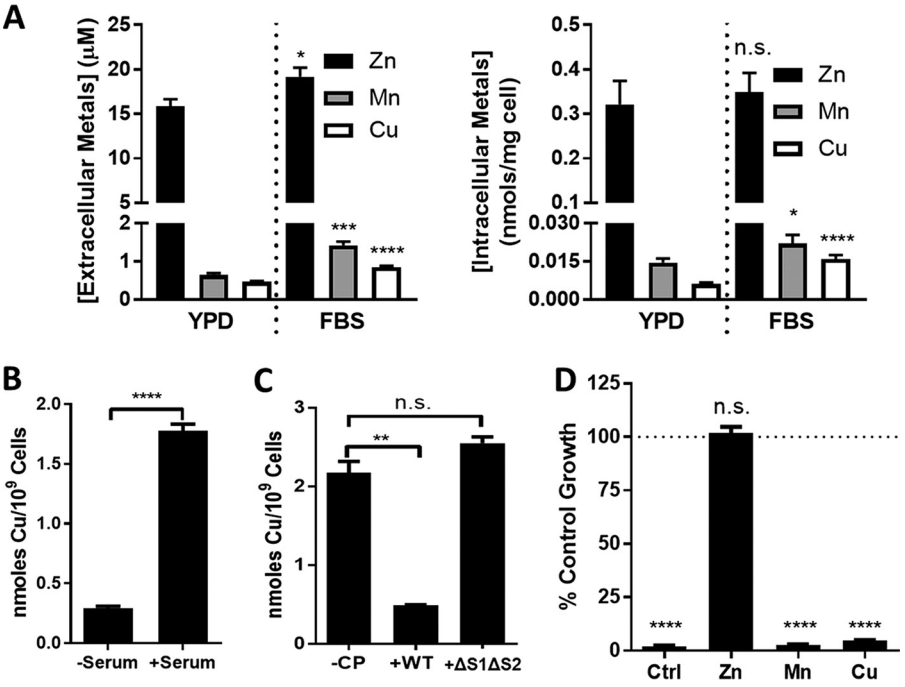

FIG 4 CP and *C. albicans* grown in serum. (A) Shown are the levels of metals in YPD medium versus the serum-based medium (FBS) as described for Fig. 3 ("extracellular metals") or the metal levels of *C. albicans* cells cultured in YPD and in FBS medium determined as described for Fig. 1C and 3B ("intracellular metals"). Error bars are standard errors for 4 to 12 biological replicates measured over two to six experimental trials. For each metal, statistical comparisons were made between FBS and YPD samples. (B and C) Total cellular Cu following 1 h of incubation with the serum-based medium or the control SC medium (−serum) (B) was analyzed as described in Materials and Methods. Where indicated (C), serum was pretreated with 1 mg ml^{-1} WT or ΔS1ΔS2 CP. Error bars are standard errors for six biological replicates (B) or biological duplicates representative of two experimental trials (C). (D) Cell growth in serum as described for Fig. 3A was carried out in the presence of 500 μg ml^{-1} CP (20 μM) and 40 μM $ZnSO_4$, $MnSO_4$, or $CuSO_4$. Error bars are standard errors for six biological replicates over three experimental trials. Statistical analyses represent comparisons to no-CP samples (dotted line).****, $P < 0.0001$; ***, $P = 0.004$; **, $P < 0.0076$; *, $P = 0.044$.

serum-grown cells involving *ZRT1* and *PRA1* (Fig. 3B). Surprisingly, however, we also observed a small but statistically significant (~2-fold) induction in the *CTR1* Cu permease gene (Fig. 3B), which was not seen in cells cultured in YPD (Fig. 1D). As previously mentioned, a major adaptation to low Cu in *C. albicans* involves Cu sparing whereby the major cuproprotein Sod1 is downregulated (7, 9). CP can induce Mn-sparing responses in *Staphylococcus aureus* (50, 51), and we tested whether the same is true for Cu sparing in *C. albicans*. In cells grown in the presence of CP, we observed an ~7-fold reduction in *SOD1* mRNA and a 15-fold increase in *SOD3* (encoding the non-Cu alternative to Sod1) (Fig. 3B). These changes indeed reflect Cu starvation stress, as we observed a 4- to 5-fold reduction in Cu when serum-grown cells were treated with 500 μg ml^{-1} CP (Fig. 3C).

The effects of CP on fungal Cu homeostasis were somewhat unexpected, as to our knowledge, there have been no prior demonstrations of CP withholding Cu from any microbial organism. As one possibility, serum might contain exceptionally high levels of Cu compared to other transition metals; however, the ratio of Cu to other metals is not dramatically different in serum versus YPD medium (Fig. 4A). In spite of the ~20-fold molar excess of Zn over Cu, CP can withhold Cu from serum-grown cells. Cu may be more bioavailable for uptake in serum, and consistent with this, *C. albicans* cells typically accumulate two to three times higher levels of Cu when grown in serum compared to YPD (Fig. 4A, right). The ability of *C. albicans* to utilize serum as a Cu source has not been previously explored, and to address this, we monitored Cu accumulation in fungal cells that were briefly exposed to 50% serum based in a low-Cu-containing synthetic medium (SC) or in SC alone. We observed that within 1 h, *C. albicans*

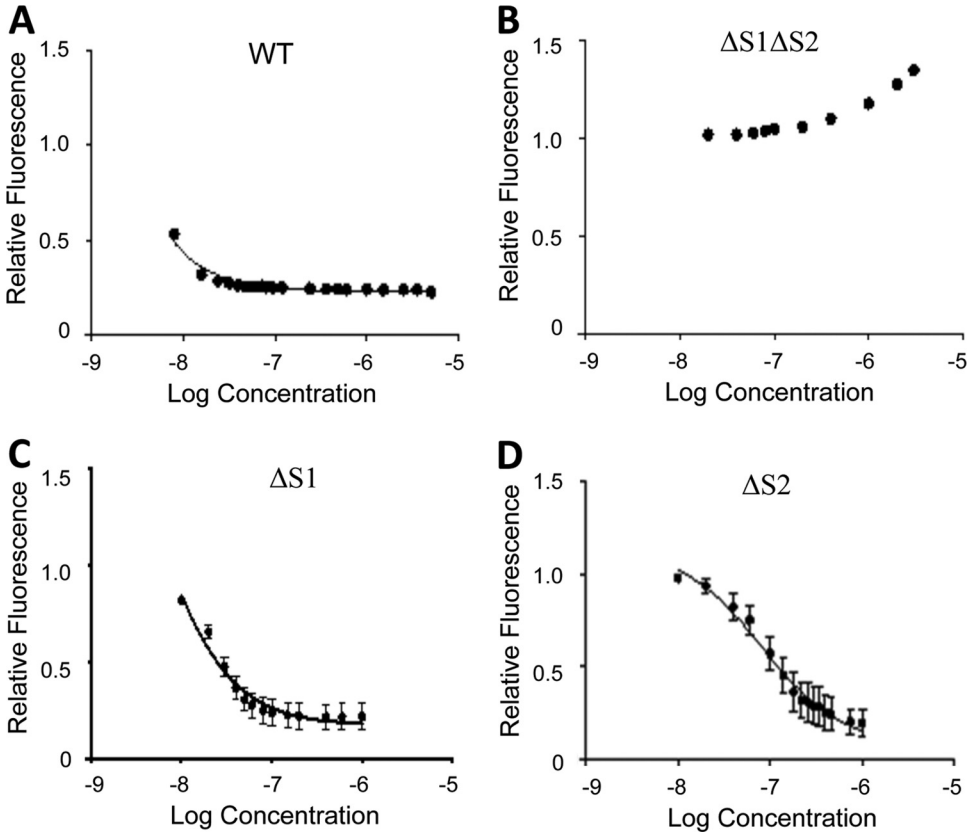

FIG 5 CP binds Cu with high affinity. Chelator competition experiments to estimate the affinity of CP for Cu were performed in triplicate as described in Materials and Methods. The binding of Cu^{2+} to WT CP-CS (A), ΔS1ΔS2 (B), ΔS1 (C), and ΔS2 (D) was assessed by tracking the change in fluorescence of Cu^{2+}-bound fluorescent chelator fluozin-3 as protein was titrated into the solution.

accumulated roughly 10-fold more Cu from serum than the SC control, demonstrating that the fungus can indeed use serum as a Cu source (Fig. 4B). Moreover, this acquisition of Cu was prevented by preincubating serum with wild-type (WT) CP, but not the ΔS1ΔS2 CP metal binding mutant (Fig. 4C). Thus, *C. albicans* can indeed acquire Cu from a source(s) in serum that is susceptible to withholding by CP.

Given the evidence for CP sequestration of Cu, we wanted to explore the ability of recombinant CP to directly bind this metal ion. The affinity of CP for Cu was determined using a competition chelator assay and the fluorescent chelator flurozin-3 (FZ3), which has high affinity for Cu^{2+} (dissociation constant [K_d] = 91 pM) (52). This assay is similar to that previously reported for measuring the affinity of CP for Zn (31). To facilitate the analysis, we used a recombinant CP lacking cysteine residues (CP-CS), which has the same biochemical and antimicrobial properties as native CP but does not require the presence of a reducing agent (31, 53). Under all conditions tested, relatively modest excesses of CP-CS were sufficient to outcompete FZ3 for its bound Cu^{2+} ions, indicating that CP binds Cu^{2+} significantly more tightly than the probe (Fig. 5A). This tight binding to Cu involves both transition metal sites, as the stoichiometry was two Cu^{2+} ions per CP heterodimer and no high-affinity binding was observed with the ΔS1ΔS2 CP mutant (Fig. 5B). To estimate the Cu^{2+} affinities for each of the two sites, we next repeated the competition chelator experiments with FZ3 using CP mutants that lack the key residues required for transition metal binding in either site 1 (ΔS1) or site 2 (ΔS2). Titrations of protein into Cu^{2+}-bound FZ3 again revealed that only modest quantities of protein were required to outcompete the chelator. Fitting of the titration data to standard binding equations provided upper limits for the K_d values for site 1 and site 2 of 4 ± 2 pM and 0.2 ± 0.1 pM, respectively (Fig. 5C and D). These values parallel those

reported for the affinity of CP for Zn (31). Hence, like Zn, CP binds Cu with high affinity using both transition metal binding sites.

Altogether, the results of our *in vitro* studies shown in Fig. 1 to 5 demonstrate that through high-affinity metal binding, CP has the capacity to withhold metals such as Zn and Cu from *C. albicans* and the fungus responds by inducing the corresponding metal starvation stress response genes. Following prolonged exposure to concentrated CP, *C. albicans* ultimately succumbs to CP toxicity, and in both YPD (Fig. 2A and B) and serum (Fig. 4D) this growth inhibition appears to involve Zn limitation since it was specifically rescued by supplementation with Zn salts. To better understand the impact of CP on *C. albicans* growth and metal homeostasis, we turned to an *in vivo* model of candidiasis.

Model of disseminated candidiasis in *S100A9*$^{-/-}$ mice. To investigate the role that CP may play in sequestering Zn and/or Cu away from *C. albicans in vivo*, we used a murine model of disseminated candidiasis in which the kidney is the main target organ. In this model, *C. albicans* is introduced into the bloodstream via a lateral tail vein injection and quickly disseminates to target organs, particularly the kidney. Kidney abscesses appear as soon as 24 h after infection, and the mice typically succumb to infection within 1 to 2 weeks (54, 55). To examine the impact of CP in this model, we used C57BL/6 *S100A9*$^{-/-}$ (CP$^{-/-}$) mice containing a homozygous deletion in the S100A9-encoding gene; the S100A8 protein is destabilized in immune cells of this mouse, leading to a CP-deficient mouse model (56).

Our studies specifically focused on the first 72 h of infection, when the host and fungal pathogen exhibit defined changes in metal homeostasis (7, 8, 10, 57). During this period, there was a continual rise in expression of S100A8 and S100A9 mRNA, indicative of increasing CP in the kidneys of WT mice (Fig. 6A). Within these first 72 h, CP$^{-/-}$ mice did not show signs of increased infection severity. WT C57BL/6 (C57) and CP$^{-/-}$ mice exhibited the same pattern of weight loss (Fig. 6B). Furthermore, kidneys of CP$^{-/-}$ mice did not exhibit any increase in CFU; if anything, the fungal burden was somewhat lower in CP$^{-/-}$ mice at 72 h (Fig. 6C) (see Discussion). In addition to weight loss and fungal burden, we monitored serum Cu levels, a biomarker of acute infection. We previously reported a progressive rise in serum Cu levels during the first 72 h of *C. albicans* infection in BALB/c mice, consistent with other models of infection and inflammation (7, 58–63). The same increase in serum Cu occurred in C57 mice during *C. albicans* infection, and there was no difference between WT C57 and CP$^{-/-}$ mice (Fig. 6D).

Cu and Zn homeostasis effects during fungal invasion of the kidney. As mentioned above, CP can sequester Cu from *C. albicans* cultured in serum, and we tested whether the same holds true *in vivo*. We and others have previously demonstrated that kidney Cu levels decrease by 72 h of *C. albicans* infection in BALB/c mice and the fungus elicits a Cu starvation stress response involving reduction in *SOD1* mRNA and a reciprocal induction of *SOD3* (7, 8), similar to the *in vitro* response that we describe here with CP (Fig. 3B). As with BALB/c mice, WT C57 mice exhibited a lowering of kidney Cu by 72 h of infection (Fig. 7A). This decrease in tissue Cu was unchanged in CP$^{-/-}$ mice, demonstrating that CP is not necessary for the global changes in kidney Cu during infection. In examining fungal mRNA, we observed that over the course of infection, *C. albicans* exhibited the transcriptional hallmark of Cu starvation: a decrease in *SOD1* (Fig. 7B) and an increase in *SOD3* expression (Fig. 7C); this fungal Cu stress response at 72 h was unaffected by CP$^{-/-}$ mutations (Fig. 7B and C). However, induction of *SOD3* at 24 h was significantly attenuated in CP$^{-/-}$ mice (Fig. 7C). Thus, CP may partly contribute to Cu withholding in the kidney, but only at early time points of infection.

We also examined fungal markers of Zn limitation stress during *C. albicans* invasion of the kidney. At 24 h, Zn-responsive genes *ZRT1* and *PRA1* increased approximately 40-fold compared to the inoculum. Interestingly, this stress response was transient, as it was greatly attenuated at 72 h postinfection (Fig. 8A and B). A similar short-lived induction of *ZRT1* and *PRA1* has also been reported for *C. albicans* invading kidneys of

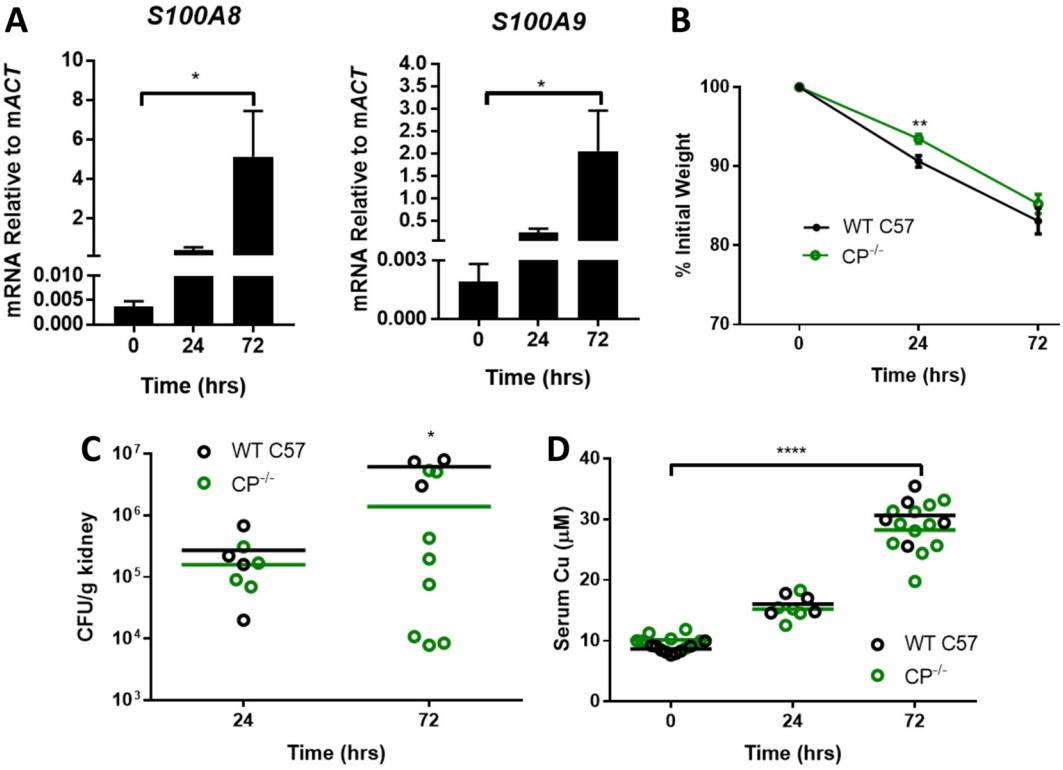

FIG 6 Disseminated candidiasis in WT C57 and CP$^{-/-}$ mice. WT C57 (black) and CP$^{-/-}$ male mice (green) were infected with *C. albicans* SC5314 via a lateral tail vein injection as described in Materials and Methods. (A) Total mRNA from uninfected and infected kidneys of WT C57 mice was subjected to qRT-PCR analysis of mouse S100A8 and S100A9 mRNA normalized to ActB mRNA. Results are the averages for four or five WT mice per time point. Expression levels increased significantly over time as determined by a one-way ANOVA with a Tukey posttest (*, $P < 0.05$). (B) Weight loss was monitored daily; results are the averages for 14 and 22 WT and CP$^{-/-}$ mice, respectively; error bars represent standard errors. CP$^{-/-}$ mice have a statistically significant lower weight loss at 24 h (**, $P = 0.004$) but not at 72 h. (C) Kidney fungal burden was determined by CFU; shown are results from three to eight independent mice per group. Bars represent averages. At 72 h postinfection, WT C57 mice have a higher fungal burden as determined by two-tailed *t* test (*, $P < 0.05$). (D) Analysis of serum Cu from 4 to 11 independent mice per group. Using a two-tailed *t* test, there was no statistical difference between WT C57 and CP$^{-/-}$ mice, but Cu levels did rise significantly during infection in both groups, as determined by a one-way ANOVA with a Tukey posttest (****, $P < 0.0001$). Bars represent averages.

BALB/c mice (11). Most importantly, the induction of *ZRT1* and *PRA1* at 24 h in WT C57 mice was essentially eliminated in the CP$^{-/-}$ mouse, as was the attenuated *PRA1* response at 72 h (Fig. 8A and B). These results demonstrate that CP acts to withhold Zn nutrients at early stages of infection and *C. albicans* adapts through a strong induction of Zn uptake systems. This induction of fungal *ZRT1* and *PRA1* may promote

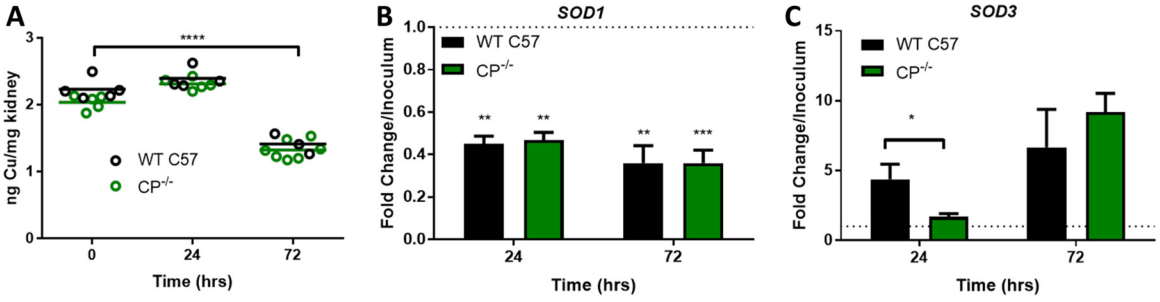

FIG 7 Host and fungal Cu responses during infection of WT and CP$^{-/-}$ mice. (A) Total kidney Cu is shown for three to seven independent mice per group. Bars represent averages. The loss in Cu at 72 h is significant (****, $P < 0.0001$), but there is no significant difference between WT and CP$^{-/-}$ mice. (B and C) Total mRNA from infected kidneys was subjected to qRT-PCR analysis of *C. albicans SOD1* (B) and *SOD3* (C). mRNA was normalized to *TUB2* and is shown as fold change over the inoculum. Results are the averages for 4 WT mice per time point and 4 or 11 CP$^{-/-}$ mice at 24 and 72 h, respectively. *SOD1* levels decreased significantly compared to the inoculum (dashed line); error bars are standard errors. The difference in *SOD3* expression between WT and CP$^{-/-}$ mice at 24 h is statistically significant. Significance was determined by one-way ANOVA with Tukey posttest (A, B) or by a two-tailed *t* test (C). **, $P < 0.01$; *, $P = 0.027$.

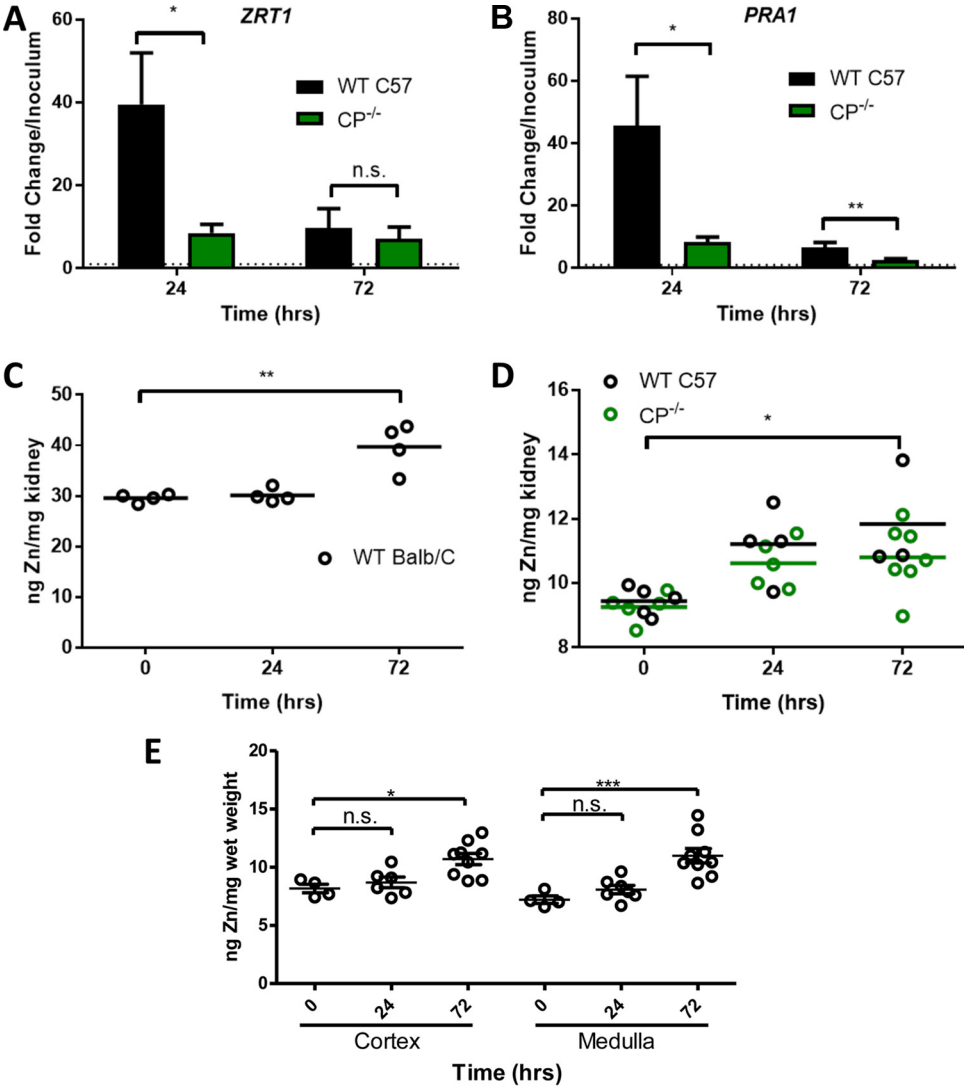

FIG 8 Host and fungal Zn responses during infection of WT and CP$^{-/-}$ mice. (A and B) Expression of *C. albicans ZRT1* (A) and *PRA1* (B) in infected kidneys was determined as described for Fig. 7B and C. Error bars represent standard errors. Significant differences between WT and CP$^{-/-}$ were determined using a two-tailed *t* test (*, $P < 0.05$). (C and D) Total Zn was measured in kidneys from uninfected mice as well as BALB/c (C) or C57 WT and CP$^{-/-}$ mice (D) at 24 h or 72 h postinfection. The increases in Zn at 72 h postinfection are statistically significant, but there is no significant difference between C57 WT and CP$^{-/-}$ mice as determined using one-way ANOVA with Tukey's posttest or a two-tailed *t* test. (E) Kidneys were dissected into cortex and medulla prior to analysis of total Zn from four uninfected and seven (24 h) or nine (72 h) infected BALB/c mice. Significance was determined by a two-tailed *t* test (A, B) or one-way ANOVA with Tukey's posttest (C to E). ***, $P < 0.001$; **, $P < 0.0074$; *, $P < 0.05$.

pathogenesis, since null mutations in the *ZAP1* regulator of these genes show evidence of causing decreased virulence in the mouse model of disseminated candidiasis (10, 64).

To probe the recovery from Zn starvation at later time points, we investigated Zn levels in the kidney. Unlike Cu, which declines in the kidney by 72 h (Fig. 7A) (7, 8), we observed an increase in total kidney Zn with both BALB/c and WT C57 mice (Fig. 8C and D). This increase in kidney Zn appears to be tissue-wide and can be observed in both the cortex and the medulla (Fig. 8E). There was no statistically significant difference between WT C57 and CP$^{-/-}$ kidneys in terms of total Zn accumulation (Fig. 8D). Together the findings shown in Fig. 8 indicate that host Zn pools are dynamic during fungal invasion. Zn availability is initially restricted by CP, followed by a rise in total kidney Zn and fungal recovery from Zn limitation stress.

DISCUSSION

The tight binding affinity of CP for divalent metal ions provides this protein with the capacity to deplete the extracellular environment of various transition metal micronutrients (6, 13–22, 31, 32, 38). With *C. albicans*, CP is highly effective at inflicting a Zn starvation stress state that involves Zn uptake by *ZRT1* and *PRA1*. With this response to CP, *C. albicans* maintains constant intracellular Zn over numerous cell divisions despite virtually undetectable bioavailable Zn outside the cell. Similar findings with Zn transporters and CP have been reported for the fungal pathogen *A. fumigatus* (17, 18), and upregulation of transition metal import genes is also an effective strategy against CP in bacterial pathogens including *Acinetobacter baumannii*, *S. aureus*, and *Salmonella* (14, 16, 20, 65, 66). Aside from Zn, we demonstrate for the first time that CP can withhold Cu from a microbial organism by virtue of its picomolar affinity for Cu(II). Specifically, CP inhibited *C. albicans* acquisition of Cu from serum source(s) of the metal.

Many studies with CP and transition metals in microbes have used *in vitro* cultures, in which, depending on the metal ion constituents of the growth medium, the effects of CP on transition metals and microbial growth can greatly vary. For example, CP is more effective at inhibiting *C. albicans* growth in a Sabouraud dextrose broth than in YPD (47), with the principal difference being the presence of yeast extract in YPD impacting metal availability. We show here that although YPD and serum have similar total transition metals, they widely vary in terms of Cu bioavailability, demonstrated by the ability of CP to withhold Cu from serum but not from YPD. Cu availability in YPD medium is particularly low, reflecting strong Cu chelating components of this complex medium (67). Typical laboratory growth media, whether they are chemically defined or more complex (e.g., YPD), cannot readily replicate the metal environment of an animal host, although animal serum is expected to contain many of the natural sources. Much of the Cu in circulatory serum is transported via the globular proteins ceruloplasmin, transcuprein, and albumin (68). Interestingly, albumin, with an affinity for Cu K_d of $\geq 10^{-11}$ M (69, 70), can directly bind *C. albicans* and serve as a nitrogen source for the fungus (71, 72) and may very well serve as a source of metals. Given the high affinity of CP for Cu ($K_d \leq 0.2 \times 10^{-12}$ M), it seems plausible that CP can compete with albumin or other serum sources of Cu to preclude Cu acquisition by *C. albicans*.

Whenever possible, it is important to validate *in vitro* findings with CP and metals with *in vivo* models of infection. We show here that during *C. albicans* invasion of the kidney, CP plays a pronounced role in withholding Zn from the fungus, as demonstrated by induction of the fungal Zn starvation stress response. *C. albicans* also exhibits a Cu limitation stress response in the kidney similar to that observed with CP-treated serum *in vitro*; however, *in vivo*, CP is not mainly responsible for limiting Cu. CP null mutations only partly attenuated the fungal Cu starvation stress response and only at early (24 h) stages of infection. Cu homeostasis in the kidney is complex and may involve local changes in Cu availability at the site of infection, as might occur with CP, as well as more-global changes in kidney Cu. At 72 h postinfection, total kidney Cu drops independent of CP. The mechanism for this total loss in Cu may involve kidney Cu exporting ATPases ATP7a or ATP7b, which have been shown by Mackie et al. to be induced during fungal infection (8).

It is curious that the effects of CP *in vivo* are transient and seen only at early stages. This is particularly obvious with Zn, as the fungal Zn stress state that is dependent on CP spikes at 24 h followed by a recovery at 72 h. This recovery does not reflect loss of CP because neutrophils continuously infiltrate the kidney throughout fungal infection (55) and CP expression continues to rise (Fig. 6A). The recovery from Zn starvation stress may reflect the strong induction of Zn acquisition systems by Pra1 and Zrt1. Alternatively, the elevation in total kidney Zn that we observe at later stages of infection may account for the recovery. The dynamics in Zn that we report here are reminiscent of what has been observed with *Streptococcus pneumoniae* infection of the lung (73). The bacteria show signs of Zn deprivation at early stages, followed by a recovery at later stages (74). With metals such as Zn and Cu that are both essential nutrients and toxic

to microbes, the host response is not one-sided and antimicrobial tactics can involve metal withholding and/or metal overload strategies (2, 6, 75–77). During fungal invasion of the kidney, it appears that both strategies are deployed and with temporally distinct signatures for Cu and Zn. The fall in kidney Cu at late stages of infection is accompanied by elevations in kidney Zn in both the cortex and the medulla. The mechanisms for Zn elevation are unknown and are the subject of ongoing investigations.

Lastly, is CP an effective anti-*Candida* agent? In *C. albicans* cultures *in vitro*, concentrated levels (≥500 μg ml^{-1}) of CP can prohibit fungal growth after prolonged incubations with CP, and our studies indicate that this growth arrest is specifically due to Zn limitation stress. Although CP can be toxic to *C. albicans in vitro*, its efficacy as an antifungal agent *in vivo* may vary depending on the host niche. For example, CP$^{-/-}$ mice are substantially more susceptible to *C. albicans* infection of the lung (26), but not to vaginal candidiasis, in spite of abundant neutrophil recruitment to the vaginal tissue (78). If anything, the opposite was observed: the fungal burden was decreased in vaginal tissues of CP$^{-/-}$ mice (78), and we observed that the same is true during fungal invasion of the kidney. This unexpected loss in fungal burden may represent compensatory mechanisms in CP$^{-/-}$ mice, in which certain immune factors are induced to correct for the deficit in CP, as has been reported for other genetic mouse models of immune deficiency (79). Our findings of a lower fungal burden in the kidneys of CP$^{-/-}$ mice appear to counter a previous report that CP$^{-/-}$ mice succumb to disseminated candidiasis infection more quickly (26). Currently, we cannot explain the discrepancy. However, the reported effects of CP$^{-/-}$ mutations on mortality were relatively mild compared to pulmonary infections examined in parallel and there were no analyses of kidney fungal burdens in that previous report (26).

Overall, our studies here highlight the role of CP as an early responder during fungal infection in limiting metal micronutrients from *C. albicans*, particularly Zn. CP is just one of many host factors at work that exploit the essential and toxic nature of transition metals, such as Zn and Cu, in antimicrobial weaponry. It will be intriguing to understand how the host orchestrates the various mechanisms for controlling metal ion dynamics at the host-fungal pathogen interface.

MATERIALS AND METHODS

Fungal strains and culture conditions. *Candida albicans* strains used in this study are SC5314 and strains derived from this isolate, including SN152 (*his1*Δ*/his1*Δ *leu2*Δ*/leu2*Δ *arg4*Δ*/arg4*Δ *URA3/ura3*Δ::*imm434 IRO1/iro1*Δ::*imm434*) and the isogenic *zap1*Δ::*LEU2/zap1*Δ::*HIS1* isolate, TF106, which were obtained from the Fungal Genetics Stock Center (64, 80). *C. albicans* was grown at 30°C in either a standard enriched medium (YPD; BD Difco) containing 1% yeast extract, 2% peptone, and 2% dextrose (wt/vol) or a medium containing 50% fetal bovine serum (FBS; Sigma) and 50% of a low-Cu SC medium prepared by using a 0.67% yeast nitrogen base without Fe or Cu (Sunrise Science), 0.2 mg/liter $FeCl_3$, and Chelex-100 treated water. For long-term growth, cells were seeded at an optical density at 600 nm (OD_{600}) of 0.005 (YPD) or 0.05 (50% FBS) and cultured for 16 h, the time point at which control cells doubled ~12 times. With serum cultures, all cells reverted to the budding/yeast form by 16 h and growth was accurately monitored by optical density. Shorter-term growth used cells seeded at an OD_{600} of 0.5 and cultured for 7 h, when cells doubled ~five times. Cultures were supplemented as indicated with recombinant WT CP or ΔS1ΔS2 CP prepared as previously described (28, 30) or with equivalent amounts of CP buffer (20 mM Tris [pH 7.5], 100 mM NaCl, 10 mM β-mercaptoethanol [BME], 3 mM $CaCl_2$).

For probing the uptake of Cu from serum, *C. albicans* cells were first starved for Cu by growing for 16 h at a starting OD_{600} of 0.005 at 30°C in low-Cu SC medium supplemented with 500 μM the Cu(I) chelator, bathocuproinesulfonate. Five to 20 OD_{600} units of cells were harvested, washed once with 10 mM Tris–1 mM EDTA, pH 8, and resuspended in low-Cu SC or the aforementioned 50% FBS medium that was pretreated for 30 min with 1 mg ml^{-1} WT CP or ΔS1ΔS2 CP or with CP buffer at 30°C. Cells were subsequently incubated for 1 h at 30°C before preparation for Cu analysis by atomic absorption spectroscopy (AAS) (see below).

Biochemical analyses. All samples of recombinant WT and mutant CP were prepared according to our standard published protocols (28, 30). For metal analysis, 5 to 10 OD_{600} cell units or 5 to 20 mg of cells were harvested and washed twice with cold 10 mM Tris–1 mM EDTA, pH 8, and twice with cold MilliQ deionized water. Cell recovery was determined by optical density and/or by weight. For AAS, 5 OD_{600} units of cells was resuspended in 1.0 ml of MilliQ deionized water and Cu content was measured on an AAnalyst600 graphite furnace atomic absorption spectrometer (PerkinElmer). For inductively coupled plasma-mass spectrometry (ICP-MS), 5 to 10 OD_{600} cell units or 5 to 20 mg cells was resuspended in 500 μl of 20% (vol/vol) Optima grade nitric acid (Fisher) and digested overnight at 90°C. The following

day, samples were diluted 1:10 with MilliQ deionized water for a final concentration of 2% nitric acid, and metal content was determined by ICP-MS (Agilent 7700x). Metal content was normalized to cell number or mass. To analyze metals in YPD medium (no cells) sequestered by CP, we adapted a filtration method of Nakashige et al. (21). Briefly, growth medium that was treated with CP or CP buffer for 7 h at 30°C was passed through a 10-kDa molecular mass cutoff Amicon Ultra centrifugal filter. The soluble filtrate lacking CP and CP-bound metals was diluted 5-fold in 2% Optima grade nitric acid (Fisher) before being subjected to ICP-MS. For metal analysis of mouse kidneys, one kidney half was weighed and dissolved in 1.0 ml of 20% (vol/vol) Optima grade nitric acid (Fisher) and digested overnight at 90°C. The following day, the samples were diluted 1:10 with MilliQ deionized water and subjected to ICP-MS.

To measure the binding of recombinant CP to Cu^{2+}, fluorescence titrations were carried out in triplicate using a Horiba Jobin Yvon Fluoromax-3 spectrofluorometer with an L-format, single cuvette holder. Temperature was regulated by a water bath kept at 22°C. The fluorometer was equipped with magnetic stirring and polarizers. All titration experiments were performed in a quartz 10-mm rectangular fluorometer cell (Starna Cells, Inc.). Prior to any titration, dialysis was carried out using 18-mm, 1.0-kDa-cutoff dialysis tubing. Dialysis was performed in 25 mM MES at pH 7.0, 100 mM NaCl, and 2 mM BME overnight at 4°C. The buffer was filtered with a 0.45-μm filter to reduce background noise in the fluorometer. After dialysis, the protein concentration was calculated using the nanophotometer and established extinction coefficients. For all titrations, a stock of CP (~300 μl total) with 100 μM CP and 400 μM Ca^{2+} was made. Increasing volumes of this CP/Ca^{2+} solution were titrated into the Starna cell containing a solution of 2.0 μM $CuSO_4$ and 2.0 μM flurozin-3 (FZ3) (initial volume present, 3,000 μl). Between titrations, 2 min of incubation was sufficient for the titrated solution to reach equilibrium. Prior to adding the FZ3 and $CuSO_4$, the initial fluorescence of the buffer alone was measured to ensure that no peaks were present prior to addition of probe and Cu^{2+} ions. For all fluorometer titrations, the instrument was set to the following: excitation wavelength, 494 nm; slit, 5.0 nm; emission wavelength, 500 to 650 nm; Inc, 1; slit width, 5.0 nm. After collecting the raw data, the fluorescence values were quantified at 517 nm. Relative intensities were calculated and plotted against the log of protein concentration. Affinities were estimated using the One Site-Ki fit in GraphPad Prism 5.

RNA analysis was carried out by qRT-PCR. With fungus-only cultures, RNA was obtained from at least five OD_{600} cell units of *C. albicans* via acid-phenol extraction as previously described (7). RNA was subsequently DNase treated using a Nucleospin RNA kit (Macherey-Nagel), and cDNA was synthesized from 1.0 μg of RNA using a RevertAid First Strand cDNA synthesis kit (Thermo Scientific). cDNA was diluted 1:10 prior to PCR analysis with iTaq Universal SYBR green Supermix (Bio-Rad), and values were normalized to *TUB2*. Relative expression was calculated using the ΔC_T method (where C_T is threshold cycle). Amplicons of ~200 bp were obtained from the following primers: *SOD1*, CTACTGATGGTAATGG TGTTGCTAA and CCAGCATGACCAGTAGTTTTAGAAT; *SOD3*, CAGTATGGGTCTGTTTCAAACCTTA and GATA TTGCAAGTAGTACGCATGTTC; *CTR1*, CAAAAGCTCGTGGAACCGGTAAATC and TCAGCAACAAATCTTCCAAC ACCGG; *ZRT1*, TGCCAGTTCCAACCAATACA and TGTCATCGACACAATGCTCA; *PRA1*, TGCACCAGTTACGGTT ACCA and CGATTTGCTACCGAATCTCA; *TUB2*, GAGTTGGTGATCAATTCAGTGCTAT and ATGGCGGCATCTTC TAATGGGATTT; ActB, GGCTGTATTCCCCTCCATCG and CCAGTTGGTAACAATGCCATGT; S100A8, AAATCAC CATGCCCTCTACAAG and CCCACTTTTATCACCATCGCAA; S100A9, CAGCATAACCACCATCATCG and GTCC TGGTTTGTGTCCAGGT. For RNA analysis of kidneys, RNA from whole kidneys was extracted and purified as previously described (7). cDNA was made from 5.0 μg of RNA and diluted 1:2 (fungal genes) or 1:50 (murine host genes) prior to PCR analysis as described above. Fold changes compared to the inoculum were calculated using the ΔC_T method. RNA from the inoculum, which was *C. albicans* grown to stationary phase in YPD and washed twice with sterile phosphate-buffered saline (PBS), was extracted and prepared using acid-phenol extraction as descried above.

Data for all studies were considered statistically significantly different for P values of ≤ 0.05 using the two-tailed t test or a one-way analysis of variance (ANOVA) with a Tukey posttest as determined by Graphpad Prism 7.

Model of disseminated candidiasis. Animal studies were carried out in accordance with the National Institutes of Health guidelines for the ethical treatment of animals. Experiments involving BALB/c mice were approved by the Institutional Animal Care and Use Committee (IACUC) of Johns Hopkins University (protocol number MO13M264). Nine-week-old female BALB/c mice were infected via a lateral tail vein injection with 5×10^5 *C. albicans* SC5314 cells in sterile PBS. The kidneys from four to nine infected mice and four uninfected controls were weighed and prepared for metal analysis as above or dissected into medulla and cortex prior to weighing and metal analysis. Experiments involving C57BL/6 mice were approved by the IACUC of the University of Illinois Urbana-Champaign (license number 16005). Nine- to 10-week-old male WT C57BL/6 or CP-deficient (C57BL/6 S100A9$^{-/-}$) mice were infected via a lateral tail vein injection as described above for BALB/c mice. Mice were monitored and weighed daily. At 24 and 72 h postinfection, 4 to 11 mice from each mouse strain were sacrificed along with uninfected controls. In the case of C57 background mice, serum was collected and organs were perfused as previously described (7). One kidney was placed in 500 μl of Trizole and flash frozen before being stored at −80°C for subsequent RNA analysis (see above). The other kidney was bisected sagitally, with one half stored at −80°C for subsequent metal analysis (see above) and the other half processed for CFUs as previously described (7).

ACKNOWLEDGMENTS

This work was supported by NIH grants R01 AI 119949 (V.C.C. and B.P.C.), F32 AI124506 (A.N.B.), F31 DK111114-01 (E.M.C.), T32 ES07141 (C.X.L.), T32 CA009110 (A.N.B.), R01 AI118880 (T.E.K.-F.), R01 AI101171 (W.J.C.), and T32 ES007028 (B.A.G.). C.R.

was supported by the Vanderbilt NSF REU in Chemical Biology. Work in the T.E.K.-F. laboratory is also supported by a Basel O'Conner Stater Scholar award from the March of Dimes.

REFERENCES

1. Lionakis MS. 2014. New insights into innate immune control of systemic candidiasis. Med Mycol 52:555–564. https://doi.org/10.1093/mmy/myu029.
2. Besold AN, Culbertson EM, Culotta VC. 2016. The Yin and Yang of copper during infection. J Biol Inorg Chem 21:137–144. https://doi.org/10.1007/s00775-016-1335-1.
3. Cassat JE, Skaar EP. 2013. Iron in infection and immunity. Cell Host Microbe 13:509–519. https://doi.org/10.1016/j.chom.2013.04.010.
4. Crawford A, Wilson D. 2015. Essential metals at the host-pathogen interface: nutritional immunity and micronutrient assimilation by human fungal pathogens. FEMS Yeast Res 15(7):fov071. https://doi.org/10.1093/femsyr/fov071.
5. Kehl-Fie TE, Skaar EP. 2010. Nutritional immunity beyond iron: a role for manganese and zinc. Curr Opin Chem Biol 14:218–224. https://doi.org/10.1016/j.cbpa.2009.11.008.
6. Subramanian Vignesh K, Deepe GS, Jr. 2016. Immunological orchestration of zinc homeostasis: the battle between host mechanisms and pathogen defenses. Arch Biochem Biophys 611:66–78. https://doi.org/10.1016/j.abb.2016.02.020.
7. Li CX, Gleason JE, Zhang SX, Bruno VM, Cormack BP, Culotta VC. 2015. Candida albicans adapts to host copper during infection by swapping metal cofactors for superoxide dismutase. Proc Natl Acad Sci U S A 112:E5336–E5342. https://doi.org/10.1073/pnas.1513447112.
8. Mackie J, Szabo EK, Urgast DS, Ballou ER, Childers DS, MacCallum DM, Feldmann J, Brown AJ. 2016. Host-imposed copper poisoning impacts fungal micronutrient acquisition during systemic Candida albicans infections. PLoS One 11:e0158683. https://doi.org/10.1371/journal.pone.0158683.
9. Broxton CN, Culotta VC. 2016. An adaptation to low copper in Candida albicans involving SOD enzymes and the alternative oxidase. PLoS One 11:e0168400. https://doi.org/10.1371/journal.pone.0168400.
10. Xu W, Solis NV, Ehrlich RL, Woolford CA, Filler SG, Mitchell AP. 2015. Activation and alliance of regulatory pathways in C. albicans during mammalian infection. PLoS Biol 13:e1002076. https://doi.org/10.1371/journal.pbio.1002076.
11. Hebecker B, Vlaic S, Conrad T, Bauer M, Brunke S, Kapitan M, Linde J, Hube B, Jacobsen ID. 2016. Dual-species transcriptional profiling during systemic candidiasis reveals organ-specific host-pathogen interactions. Sci Rep 6:36055. https://doi.org/10.1038/srep36055.
12. Nobile CJ, Nett JE, Hernday AD, Homann OR, Deneault JS, Nantel A, Andes DR, Johnson AD, Mitchell AP. 2009. Biofilm matrix regulation by Candida albicans Zap1. PLoS Biol 7:e1000133. https://doi.org/10.1371/journal.pbio.1000133.
13. Corbin BD, Seeley EH, Raab A, Feldmann J, Miller MR, Torres VJ, Anderson KL, Dattilo BM, Dunman PM, Gerads R, Caprioli RM, Nacken W, Chazin WJ, Skaar EP. 2008. Metal chelation and inhibition of bacterial growth in tissue abscesses. Science 319:962–965. https://doi.org/10.1126/science.1152449.
14. Hood MI, Mortensen BL, Moore JL, Zhang Y, Kehl-Fie TE, Sugitani N, Chazin WJ, Caprioli RM, Skaar EP. 2012. Identification of an Acinetobacter baumannii zinc acquisition system that facilitates resistance to calprotectin-mediated zinc sequestration. PLoS Pathog 8:e1003068. https://doi.org/10.1371/journal.ppat.1003068.
15. Gaddy JA, Radin JN, Cullen TW, Chazin WJ, Skaar EP, Trent MS, Algood HM. 2015. Helicobacter pylori resists the antimicrobial activity of calprotectin via lipid A modification and associated biofilm formation. mBio 6:e01349-15. https://doi.org/10.1128/mBio.01349-15.
16. Juttukonda LJ, Chazin WJ, Skaar EP. 2016. Acinetobacter baumannii coordinates urea metabolism with metal import to resist host-mediated metal limitation. mBio 7(5):e01475-16. https://doi.org/10.1128/mBio.01475-16.
17. Clark HL, Jhingran A, Sun Y, Vareechon C, de Jesus Carrion S, Skaar EP, Chazin WJ, Calera JA, Hohl TM, Pearlman E. 2016. Zinc and manganese chelation by neutrophil S100A8/A9 (calprotectin) limits extracellular Aspergillus fumigatus hyphal growth and corneal infection. J Immunol 196:336–344. https://doi.org/10.4049/jimmunol.1502037.
18. Amich J, Vicentefranqueira R, Mellado E, Ruiz-Carmuega A, Leal F, Calera JA. 2014. The ZrfC alkaline zinc transporter is required for Aspergillus fumigatus virulence and its growth in the presence of the Zn/Mn-chelating protein calprotectin. Cell Microbiol 16:548–564. https://doi.org/10.1111/cmi.12238.
19. Kelliher JL, Kehl-Fie TE. 2016. Competition for manganese at the host-pathogen interface. Prog Mol Biol Transl Sci 142:1–25. https://doi.org/10.1016/bs.pmbts.2016.05.002.
20. Kehl-Fie TE, Zhang Y, Moore JL, Farrand AJ, Hood MI, Rathi S, Chazin WJ, Caprioli RM, Skaar EP. 2013. MntABC and MntH contribute to systemic Staphylococcus aureus infection by competing with calprotectin for nutrient manganese. Infect Immun 81:3395–3405. https://doi.org/10.1128/IAI.00420-13.
21. Nakashige TG, Zhang B, Krebs C, Nolan EM. 2015. Human calprotectin is an iron-sequestering host-defense protein. Nat Chem Biol 11:765–771. https://doi.org/10.1038/nchembio.1891.
22. Nakashige TG, Zygiel EM, Drennan CL, Nolan EM. 2017. Nickel sequestration by the host-defense protein human calprotectin. J Am Chem Soc 139:8828–8838. https://doi.org/10.1021/jacs.7b01212.
23. Gebhardt C, Nemeth J, Angel P, Hess J. 2006. S100A8 and S100A9 in inflammation and cancer. Biochem Pharmacol 72:1622–1631. https://doi.org/10.1016/j.bcp.2006.05.017.
24. Clohessy PA, Golden BE. 1995. Calprotectin-mediated zinc chelation as a biostatic mechanism in host defence. Scand J Immunol 42:551–556. https://doi.org/10.1111/j.1365-3083.1995.tb03695.x.
25. Fuchs TA, Abed U, Goosmann C, Hurwitz R, Schulze I, Wahn V, Weinrauch Y, Brinkmann V, Zychlinsky A. 2007. Novel cell death program leads to neutrophil extracellular traps. J Cell Biol 176:231–241. https://doi.org/10.1083/jcb.200606027.
26. Urban CF, Ermert D, Schmid M, Abu-Abed U, Goosmann C, Nacken W, Brinkmann V, Jungblut PR, Zychlinsky A. 2009. Neutrophil extracellular traps contain calprotectin, a cytosolic protein complex involved in host defense against Candida albicans. PLoS Pathog 5:e1000639. https://doi.org/10.1371/journal.ppat.1000639.
27. Hood MI, Skaar EP. 2012. Nutritional immunity: transition metals at the pathogen-host interface. Nat Rev Microbiol 10:525–537. https://doi.org/10.1038/nrmicro2836.
28. Damo SM, Kehl-Fie TE, Sugitani N, Holt ME, Rathi S, Murphy WJ, Zhang Y, Betz C, Hench L, Fritz G, Skaar EP, Chazin WJ. 2013. Molecular basis for manganese sequestration by calprotectin and roles in the innate immune response to invading bacterial pathogens. Proc Natl Acad Sci U S A 110:3841–3846. https://doi.org/10.1073/pnas.1220341110.
29. Brophy MB, Nakashige TG, Gaillard A, Nolan EM. 2013. Contributions of the S100A9 C-terminal tail to high-affinity Mn(II) chelation by the host-defense protein human calprotectin. J Am Chem Soc 135:17804–17817. https://doi.org/10.1021/ja407147d.
30. Kehl-Fie TE, Chitayat S, Hood MI, Damo S, Restrepo N, Garcia C, Munro KA, Chazin WJ, Skaar EP. 2011. Nutrient metal sequestration by calprotectin inhibits bacterial superoxide defense, enhancing neutrophil killing of Staphylococcus aureus. Cell Host Microbe 10:158–164. https://doi.org/10.1016/j.chom.2011.07.004.
31. Brophy MB, Hayden JA, Nolan EM. 2012. Calcium ion gradients modulate the zinc affinity and antibacterial activity of human calprotectin. J Am Chem Soc 134:18089–18100. https://doi.org/10.1021/ja307974e.
32. Nakashige TG, Stephan JR, Cunden LS, Brophy MB, Wommack AJ, Keegan BC, Shearer JM, Nolan EM. 2016. The hexahistidine motif of host-defense protein human calprotectin contributes to zinc withholding and its functional versatility. J Am Chem Soc 138:12243–12251. https://doi.org/10.1021/jacs.6b06845.
33. Gagnon DM, Brophy MB, Bowman SE, Stich TA, Drennan CL, Britt RD, Nolan EM. 2015. Manganese binding properties of human calprotectin under conditions of high and low calcium: X-ray crystallographic and advanced electron paramagnetic resonance spectroscopic analysis. J Am Chem Soc 137:3004–3016. https://doi.org/10.1021/ja512204s.
34. Hayden JA, Brophy MB, Cunden LS, Nolan EM. 2013. High-affinity manganese coordination by human calprotectin is calcium-dependent and

requires the histidine-rich site formed at the dimer interface. J Am Chem Soc 135:775–787. https://doi.org/10.1021/ja3096416.
35. Baker TM, Nakashige TG, Nolan EM, Neidig ML. 2017. Magnetic circular dichroism studies of iron(II) binding to human calprotectin. Chem Sci 8:1369–1377. https://doi.org/10.1039/C6SC03487J.
36. Kerkhoff C, Vogl T, Nacken W, Sopalla C, Sorg C. 1999. Zinc binding reverses the calcium-induced arachidonic acid-binding capacity of the S100A8/A9 protein complex. FEBS Lett 460:134–138. https://doi.org/10.1016/S0014-5793(99)01322-8.
37. Arnesano F, Banci L, Bertini I, Fantoni A, Tenori L, Viezzoli MS. 2005. Structural interplay between calcium(II) and copper(II) binding to S100A13 protein. Angew Chem Int Ed Engl 44:6341–6344. https://doi.org/10.1002/anie.200500540.
38. Gilston BA, Skaar EP, Chazin WJ. 2016. Binding of transition metals to S100 proteins. Sci China Life Sci 59:792–801. https://doi.org/10.1007/s11427-016-5088-4.
39. Moroz OV, Antson AA, Grist SJ, Maitland NJ, Dodson GG, Wilson KS, Lukanidin E, Bronstein IB. 2003. Structure of the human S100A12-copper complex: implications for host-parasite defence. Acta Crystallogr D Biol Crystallogr 59:859–867. https://doi.org/10.1107/S0907444903004700.
40. Nishikawa T, Lee IS, Shiraishi N, Ishikawa T, Ohta Y, Nishikimi M. 1997. Identification of S100b protein as copper-binding protein and its suppression of copper-induced cell damage. J Biol Chem 272:23037–23041. https://doi.org/10.1074/jbc.272.37.23037.
41. Sohnle PG, Collins-Lech C, Wiessner JH. 1991. The zinc-reversible antimicrobial activity of neutrophil lysates and abscess fluid supernatants. J Infect Dis 164:137–142. https://doi.org/10.1093/infdis/164.1.137.
42. Sohnle PG, Hahn BL, Santhanagopalan V. 1996. Inhibition of Candida albicans growth by calprotectin in the absence of direct contact with the organisms. J Infect Dis 174:1369–1372. https://doi.org/10.1093/infdis/174.6.1369.
43. Steinbakk M, Naess-Andresen CF, Lingaas E, Dale I, Brandtzaeg P, Fagerhol MK. 1990. Antimicrobial actions of calcium binding leucocyte L1 protein, calprotectin. Lancet 336:763–765. https://doi.org/10.1016/0140-6736(90)93237-J.
44. Murthy AR, Lehrer RI, Harwig SS, Miyasaki KT. 1993. In vitro candidastatic properties of the human neutrophil calprotectin complex. J Immunol 151:6291–6301.
45. Kim MJ, Kil M, Jung JH, Kim J. 2008. Roles of Zinc-responsive transcription factor Csr1 in filamentous growth of the pathogenic yeast Candida albicans. J Microbiol Biotechnol 18:242–247.
46. Citiulo F, Jacobsen ID, Miramon P, Schild L, Brunke S, Zipfel P, Brock M, Hube B, Wilson D. 2012. Candida albicans scavenges host zinc via Pra1 during endothelial invasion. PLoS Pathog 8:e1002777. https://doi.org/10.1371/journal.ppat.1002777.
47. Sohnle PG, Hunter MJ, Hahn B, Chazin WJ. 2000. Zinc-reversible antimicrobial activity of recombinant calprotectin (migration inhibitory factor-related proteins 8 and 14). J Infect Dis 182:1272–1275. https://doi.org/10.1086/315810.
48. Vogl T, Leukert N, Barczyk K, Strupat K, Roth J. 2006. Biophysical characterization of S100A8 and S100A9 in the absence and presence of bivalent cations. Biochim Biophys Acta 1763:1298–1306. https://doi.org/10.1016/j.bbamcr.2006.08.028.
49. Stephan JR, Nolan EM. 2016. Calcium-induced tetramerization and zinc chelation shield human calprotectin from degradation by host and bacterial extracellular proteases. Chem Sci 7:1962–1975. https://doi.org/10.1039/C5SC03287C.
50. Garcia YM, Barwinska-Sendra A, Tarrant E, Skaar EP, Waldron KJ, Kehl-Fie TE. 2017. A superoxide dismutase capable of functioning with iron or manganese promotes the resistance of Staphylococcus aureus to calprotectin and nutritional immunity. PLoS Pathog 13:e1006125. https://doi.org/10.1371/journal.ppat.1006125.
51. Radin JN, Kelliher JL, Parraga Solorzano PK, Kehl-Fie TE. 2016. The two-component system ArlRS and alterations in metabolism enable Staphylococcus aureus to resist calprotectin-induced manganese starvation. PLoS Pathog 12:e1006040. https://doi.org/10.1371/journal.ppat.1006040.
52. Zhao J, Bertoglio BA, Devinney MJ, Jr, Dineley KE, Kay AR. 2009. The interaction of biological and noxious transition metals with the zinc probes FluoZin-3 and Newport Green. Anal Biochem 384:34–41. https://doi.org/10.1016/j.ab.2008.09.019.
53. Hunter MJ, Chazin WJ. 1998. High level expression and dimer characterization of the S100 EF-hand proteins, migration inhibitory factor-related proteins 8 and 14. J Biol Chem 273:12427–12435. https://doi.org/10.1074/jbc.273.20.12427.
54. Clancy CJ, Cheng S, Nguyen MH. 2009. Animal models of candidiasis. Methods Mol Biol 499:65–76. https://doi.org/10.1007/978-1-60327-151-6_8.
55. Lionakis MS, Lim JK, Lee CC, Murphy PM. 2011. Organ-specific innate immune responses in a mouse model of invasive candidiasis. J Innate Immun 3:180–199. https://doi.org/10.1159/000321157.
56. Manitz MP, Horst B, Seeliger S, Strey A, Skryabin BV, Gunzer M, Frings W, Schonlau F, Roth J, Sorg C, Nacken W. 2003. Loss of S100A9 (MRP14) results in reduced interleukin-8-induced CD11b surface expression, a polarized microfilament system, and diminished responsiveness to chemoattractants in vitro. Mol Cell Biol 23:1034–1043. https://doi.org/10.1128/MCB.23.3.1034-1043.2003.
57. Potrykus J, Stead D, Maccallum DM, Urgast DS, Raab A, van Rooijen N, Feldmann J, Brown AJ. 2013. Fungal iron availability during deep seated candidiasis is defined by a complex interplay involving systemic and local events. PLoS Pathog 9:e1003676. https://doi.org/10.1371/journal.ppat.1003676.
58. Ding C, Festa RA, Chen YL, Espart A, Palacios O, Espin J, Capdevila M, Atrian S, Heitman J, Thiele DJ. 2013. Cryptococcus neoformans copper detoxification machinery is critical for fungal virulence. Cell Host Microbe 13:265–276. https://doi.org/10.1016/j.chom.2013.02.002.
59. Ilback NG, Frisk P, Tallkvist J, Gadhasson IL, Blomberg J, Friman G. 2008. Gastrointestinal uptake of trace elements are changed during the course of a common human viral (Coxsackievirus B3) infection in mice. J Trace Elem Med Biol 22:120–130. https://doi.org/10.1016/j.jtemb.2007.12.001.
60. Moreno T, Artacho R, Navarro M, Perez A, Ruiz-Lopez MD. 1998. Serum copper concentration in HIV-infection patients and relationships with other biochemical indices. Sci Total Environ 217:21–26. https://doi.org/10.1016/S0048-9697(98)00158-2.
61. Cernat RI, Mihaescu T, Vornicu M, Vione D, Olariu RI, Arsene C. 2011. Serum trace metal and ceruloplasmin variability in individuals treated for pulmonary tuberculosis. Int J Tuberc Lung Dis 15:1239–1245, i. https://doi.org/10.5588/ijtld.10.0445.
62. Kocyigit A, Erel O, Gurel MS, Avci S, Aktepe N. 1998. Alterations of serum selenium, zinc, copper, and iron concentrations and some related antioxidant enzyme activities in patients with cutaneous leishmaniasis. Biol Trace Elem Res 65:271–281. https://doi.org/10.1007/BF02789102.
63. Wisniewska M, Cremer M, Wiehe L, Becker NP, Rijntjes E, Martitz J, Renko K, Buhrer C, Schomburg L. 2017. Copper to zinc ratio as disease biomarker in neonates with early-onset congenital infections. Nutrients 9(4):E343. https://doi.org/10.3390/nu9040343.
64. Noble SM, French S, Kohn LA, Chen V, Johnson AD. 2010. Systematic screens of a Candida albicans homozygous deletion library decouple morphogenetic switching and pathogenicity. Nat Genet 42:590–598. https://doi.org/10.1038/ng.605.
65. Diaz-Ochoa VE, Lam D, Lee CS, Klaus S, Behnsen J, Liu JZ, Chim N, Nuccio SP, Rathi SG, Mastroianni JR, Edwards RA, Jacobo CM, Cerasi M, Battistoni A, Ouellette AJ, Goulding CW, Chazin WJ, Skaar EP, Raffatellu M. 2016. Salmonella mitigates oxidative stress and thrives in the inflamed gut by evading calprotectin-mediated manganese sequestration. Cell Host Microbe 19:814–825. https://doi.org/10.1016/j.chom.2016.05.005.
66. Liu JZ, Jellbauer S, Poe AJ, Ton V, Pesciaroli M, Kehl-Fie TE, Restrepo NA, Hosking MP, Edwards RA, Battistoni A, Pasquali P, Lane TE, Chazin WJ, Vogl T, Roth J, Skaar EP, Raffatellu M. 2012. Zinc sequestration by the neutrophil protein calprotectin enhances Salmonella growth in the inflamed gut. Cell Host Microbe 11:227–239. https://doi.org/10.1016/j.chom.2012.01.017.
67. Adamo GM, Brocca S, Passolunghi S, Salvato B, Lotti M. 2012. Laboratory evolution of copper tolerant yeast strains. Microb Cell Fact 11:1. https://doi.org/10.1186/1475-2859-11-1.
68. Linder MC. 2016. Ceruloplasmin and other copper binding components of blood plasma and their functions: an update. Metallomics 8:887–905. https://doi.org/10.1039/C6MT00103C.
69. Masuoka J, Hegenauer J, Van Dyke BR, Saltman P. 1993. Intrinsic stoichiometric equilibrium constants for the binding of zinc(II) and copper(II) to the high affinity site of serum albumin. J Biol Chem 268:21533–21537.
70. Masuoka J, Saltman P. 1994. Zinc(II) and copper(II) binding to serum albumin. A comparative study of dog, bovine, and human albumin. J Biol Chem 269:25557–25561.
71. Ramachandra S, Linde J, Brock M, Guthke R, Hube B, Brunke S. 2014. Regulatory networks controlling nitrogen sensing and uptake in Can-

dida albicans. PLoS One 9:e92734. https://doi.org/10.1371/journal.pone.0092734.
72. Page S, Odds FC. 1988. Binding of plasma proteins to Candida species in vitro. J Gen Microbiol 134:2693–2702.
73. McDevitt CA, Ogunniyi AD, Valkov E, Lawrence MC, Kobe B, McEwan AG, Paton JC. 2011. A molecular mechanism for bacterial susceptibility to zinc. PLoS Pathog 7:e1002357. https://doi.org/10.1371/journal.ppat.1002357.
74. Plumptre CD, Eijkelkamp BA, Morey JR, Behr F, Counago RM, Ogunniyi AD, Kobe B, O'Mara ML, Paton JC, McDevitt CA. 2014. AdcA and AdcAII employ distinct zinc acquisition mechanisms and contribute additively to zinc homeostasis in Streptococcus pneumoniae. Mol Microbiol 91:834–851. https://doi.org/10.1111/mmi.12504.
75. Ong CL, Gillen CM, Barnett TC, Walker MJ, McEwan AG. 2014. An antimicrobial role for zinc in innate immune defense against group A streptococcus. J Infect Dis 209:1500–1508. https://doi.org/10.1093/infdis/jiu053.
76. White C, Lee J, Kambe T, Fritsche K, Petris MJ. 2009. A role for the ATP7A copper-transporting ATPase in macrophage bactericidal activity. J Biol Chem 284:33949–33956. https://doi.org/10.1074/jbc.M109.070201.
77. Botella H, Peyron P, Levillain F, Poincloux R, Poquet Y, Brandli I, Wang C, Tailleux L, Tilleul S, Charriere GM, Waddell SJ, Foti M, Lugo-Villarino G, Gao Q, Maridonneau-Parini I, Butcher PD, Castagnoli PR, Gicquel B, de Chastellier C, Neyrolles O. 2011. Mycobacterial p(1)-type ATPases mediate resistance to zinc poisoning in human macrophages. Cell Host Microbe 10:248–259. https://doi.org/10.1016/j.chom.2011.08.006.
78. Yano J, Palmer GE, Eberle KE, Peters BM, Vogl T, McKenzie AN, Fidel PL, Jr. 2014. Vaginal epithelial cell-derived S100 alarmins induced by Candida albicans via pattern recognition receptor interactions are sufficient but not necessary for the acute neutrophil response during experimental vaginal candidiasis. Infect Immun 82:783–792. https://doi.org/10.1128/IAI.00861-13.
79. Nish S, Medzhitov R. 2011. Host defense pathways: role of redundancy and compensation in infectious disease phenotypes. Immunity 34:629–636. https://doi.org/10.1016/j.immuni.2011.05.009.
80. McCluskey K, Wiest A, Plamann M. 2010. The Fungal Genetics Stock Center: a repository for 50 years of fungal genetics research. J Biosci 35:119–126. https://doi.org/10.1007/s12038-010-0014-6.